The Journal of Immunology

Lipid Raft-Independent B Cell Receptor-Mediated Antigen Internalization and Intracellular Trafficking

Michelle A. Putnam, Amy E. Moquin, Megan Merrihew, Christopher Outcalt, Emily Sorge, Adriana Caballero, Timothy A. Gondré-Lewis and James R. Drake

J Immunol 2003; 170:905-912; ;
doi: 10.4049/jimmunol.170.2.905
http://www.jimmunol.org/content/170/2/905

The Journal of Immunology is published twice each month by
The American Association of Immunologists, Inc.,
1451 Rockville Pike, Suite 650, Rockville, MD 20852

Print ISSN: 0022-1767 Online ISSN: 1550-6606.

Lipid Raft-Independent B Cell Receptor-Mediated Antigen Internalization and Intracellular Trafficking[1]

Michelle A. Putnam,[2]* Amy E. Moquin,[2†] Megan Merrihew,[†] Christopher Outcalt,[†] Emily Sorge,* Adriana Caballero,* Timothy A. Gondré-Lewis[‡] and James R. Drake[3]*[†§]

The Ag-specific B cell receptor (BCR) expressed by B lymphocytes has two distinct functions upon interaction with cognate Ag: signal transduction (generation of intracellular second messenger molecules) and Ag internalization for subsequent processing and presentation. While it is known that plasma membrane domains, termed lipid rafts, are involved in BCR-mediated signal transduction, the precise role of plasma membrane lipid rafts in BCR-mediated Ag internalization and intracellular trafficking is presently unclear. Using a highly characterized model system, it was determined that while plasma membrane lipid rafts can be internalized by B lymphocytes, lipid rafts do not represent a major pathway for the rapid and efficient internalization of cell surface Ag-BCR complexes. Moreover, internalized plasma membrane lipid rafts are delivered to intracellular compartments distinct from those to which the bulk of internalized Ag-BCR complexes are delivered. These results demonstrate that B lymphocytes, like other cell types, possess at least two distinct endocytic pathways (i.e., clathrin-coated pits and plasma membrane lipid rafts) that deliver internalized ligands to distinct intracellular compartments. Furthermore, Ag-BCR complexes differentially access these two distinct internalization pathways. ***The Journal of Immunology,*** **2003, 170: 905–912.**

The plasma membrane of many cell types, including B lymphocytes, is known to contain distinct lipid domains with unique biochemical and biophysical characteristics. These lipid domains, termed lipid rafts, are known to be critically involved in signal transduction and generation of intracellular second messenger molecules in a number of different receptor systems (1, 2). The B cell receptor (BCR)[4] is a cell surface transmembrane protein that has two distinct functions upon interaction with its ligand, cognate Ag. One function of the BCR is signal transduction, which results in the generation of intracellular second messenger molecules. The second function of the BCR is to mediate the internalization and subsequent processing of bound Ag. While a role for plasma membrane lipid rafts in BCR-mediated B cell signaling appears clear (2–4), the precise role of plasma membrane lipid rafts in BCR-mediated Ag internalization and processing is presently unclear.

In many cases the internalization and intracellular trafficking of plasma membrane lipid rafts occurs via caveoli, structures that are distinct from the clathrin-coated pits that mediate the internalization of a wide range of transmembrane proteins (5–7). However, even in cells such as lymphocytes that do not produce the protein caveolin and therefore do not form caveoli (8), plasma membrane lipid rafts can be internalized by a pathway distinct from clathrin-coated pit-mediated internalization (9). While lymphocyte transmembrane molecules such as BCR (10), the B2 isoform of FcγRII (11, 12), mannose-6-phosphate receptor (13), MHC class II molecules (14), CD4 (15, 16), CTLA-4 (17–20), and TCR (18, 21) are known to be internalized via plasma membrane clathrin-coated pits, GPI-linked proteins such as CD59 are internalized in lipid rafts via a distinct pathway (9). Moreover, altered CD4 or BCR molecules, manipulated such that these normally transmembrane proteins are instead GPI-linked, efficiently partition into plasma membrane lipid rafts (22, 23) and are internalized via a non-clathrin-coated pit-mediated pathway with distinct internalization and recycling kinetics (24–26).

Recently, it has been reported that Ag-BCR complexes resident within plasma membrane lipid rafts can be internalized and delivered to endocytic compartments (22). However, this report did not address whether lipid rafts represent a major conduit for Ag-BCR endocytosis or, rather, a pathway for the internalization of a small fraction of Ag-BCR complexes. Therefore, we have more precisely analyzed the role of plasma membrane lipid rafts in the endocytosis and intracellular trafficking of Ag-BCR complexes. The results of this analysis demonstrate that while internalization of lipid raft resident Ag-BCR complexes is likely to occur, plasma membrane lipid rafts are not a major pathway for the internalization of cell surface Ag-BCR complexes. Moreover, the results demonstrate that the bulk of internalized plasma membrane lipid rafts are delivered to endocytic compartments distinct from that to which the bulk of internalized Ag-BCR complexes are delivered for subsequent Ag processing.

*Center for Immunology and Microbial Disease, Albany Medical College, Albany, NY 12208; †Trudeau Institute, Saranac Lake, NY 12983; and ‡Department of Natural Sciences-Biology, York College of The City University of New York, Jamaica, NY 11451

Received for publication October 11, 2002. Accepted for publication November 5, 2002.

The costs of publication of this article were defrayed in part by the payment of page charges. This article must therefore be hereby marked *advertisement* in accordance with 18 U.S.C. Section 1734 solely to indicate this fact.

[1] This work was supported in part by grants (to J.R.D.) from the U.S. Public Health Service (AI40236) and Trudeau Institute. T.A.G.-L. was supported by a United Negro College Fund–Parke-Davis Postdoctoral Fellowship. M.M. and C.O. were supported by Trudeau Institute's Summer Intern Program.

[2] M.A.P. and A.E.M. contributed equally to this work.

[3] Address correspondence and reprint requests to Dr. James R. Drake, Center for Immunology and Microbial Disease, Albany Medical College, 47 New Scotland Avenue, Mail Code 151, Albany, New York 12208-3479. E-mail address: drakej@mail.amc.edu

[4] Abbreviations used in this paper: BCR, B cell receptor; btn, biotin; CTB, cholera toxin B subunit; CTB-HRP, HRP-labeled cholera toxin B subunit; DAB, diaminobenzidene; DAPI, 4′,6-diamidino-2-phenylindole; DIG, digoxigenin; KLH, keyhole limpet hemocyanin; LAMP, lysosome-associated membrane protein; MBCD, methyl-β-cyclodextrin; PC, phosphorylcholine; PC-BSA, phosphorylcholine-modified BSA; PC-BSA-HRP, HRP-labeled PC-modified BSA; PC-KLH-btn, btn-labeled PC-modified keyhole limpet hemocyanin; PC-KLH-DIG, DIG-labeled PC-modified KLH; SA, streptavidin; Tf, transferrin; TfR, Tf receptor; TX-100, Triton X-100.

0022-1767/03/$02.00

Materials and Methods

Cells

The murine A20μWT and A20μPI B cell lines expressing a transfected, phosphorylcholine-specific human IgM BCR were maintained in culture in αMEM, 5% FBS, and 50 μM 2-ME (αMEM/5% FBS) as previously described (27).

Ligands

Cholera toxin B subunit (CTB)-HRP and CTB-FITC were purchased from Sigma-Aldrich (St. Louis, MO; catalog no. C-4672 and C-1655, respectively). Phosphorylcholine-modified BSA labeled with HRP (PC-BSA-HRP) was synthesized and used as previously described (27). PC-keyhole limpet hemocyanin (KLH)-digoxigenin (DIG) was generated by DIG-modifying PC-KLH using DIG-3-*O*-methylcarbonyl-ϵ-aminocaproic acid-*N*-hydroxy succinimide ester (Roche, Indianapolis, IN; catalog no. 1333054) according to the manufacturer's instructions. PC-KLH-btn was generated by biotin (btn)-modifying PC-KLH using sulfosuccinimidyl-6-(biotinamido)hexanoate (sulfo-NHS-LC-biotin; Pierce Chemical Co., Rockford, IL; catalog no. 21335) according to the manufacturer's instructions. Unconjugated DIG or btn was removed by exhaustive dialysis.

Lipid raft isolation

Lipid rafts were isolated from detergent lysates of A20μWT and A20μPI cells by sucrose density gradient centrifugation essentially as previously described (22). Specifically, cells were resuspended to a concentration of 10^8 viable cells/ml in ice-cold TNE (10 mM Tris (pH 7.5), 150 mM NaCl, and 5 mM EDTA) containing 0.1–1% Triton X-100 (TX-100; as indicated in each experimental protocol) and incubated for 30 min on ice. After clearing by centrifugation for 3 min at 1,000 $\times$ *g*, the lysate was brought to 37.5% sucrose by the addition of 3 vol of TNE/50% sucrose. The sample was then overlaid with 4 ml of TNE/30% sucrose, followed by 4 ml TNE/5% sucrose. The gradient was spun for 20 h at 35,000 rpm in an SW-41Ti rotor at 4°C. Finally, 0.5-ml fractions were collected from top to bottom on the gradient.

HRP-labeled ligand endocytosis

CTB-HRP was bound to A20μWT or A20μPI cells by incubation of the cells in 0.1 μg/ml of CTB-HRP for 30 min on ice. PC-BSA-HRP was used as previously reported (27). The kinetics of internalization of CTB-HRP and PC-BSA-HRP by A20μWT cells were determined using a colorometric assay for HRP activity as previously described (28).

Lipid raft disruption by cholesterol depletion with methyl-β-cyclodextrin (MBCD)

To deplete cellular cholesterol and disrupt lipid rafts, A20μWT B cells were treated with the indicated concentration of MBCD (Sigma-Aldrich; catalog no. C-4555) for 30 min at 37°C in αMEM/5% FBS. The level of lipid raft disruption was determined by subsequent binding of CTB-HRP to the cells and determining the fraction of cell-associated CTB-HRP that could be isolated with plasma membrane lipid rafts via sucrose density gradient centrifugation. Under these conditions, treatment with 1–5 mM MBCD resulted in the disruption of 50–80% of plasma membrane lipid rafts.

Analysis of BCR endocytosis by flow cytometry

A20μWT B cells were pulsed with 0.1–1.0 μM PC-KLH-btn on ice and then washed. The PC-KLH-btn-pulsed cells were incubated at 37°C for the indicated time and then returned to ice. The cells were stained with FITC-labeled streptavidin (SA-FITC; BD PharMingen, San Diego, CA; catalog no. 554060; at a 1:250 dilution) following washing and staining with 1 μg/ml propidium iodide. The cells were analyzed by flow cytometry using a FACScan I (BD Biosciences, San Jose, CA). The level of SA-FITC was determined by analysis of the data using the CellQuest software package (BD Biosciences) to determine the mean fluorescence intensity of FL-1 staining on live (i.e., propidium iodide-negative) cells.

Analysis of intracellular Ca^{2+} flux

A20μWT B cells were labeled for 40 min at 37°C at a concentration of 10^6 viable cells/ml with 2 μg/ml Fluo-3/AM (Molecular Probes, Eugene, OR; catalog no. F-1242) and 5 μg/ml Fura Red/AM (Molecular Probes; catalog no. F-3021) in HBSS containing 1% FBS, 1 mM Ca^{2+}, 1 mM Mg^{2+}, and 4 mM probenecid (loading buffer). The cells were then washed, resuspended to a concentration of 2×10^6 viable cells/ml in loading buffer, and rested for 2 h at room temperature before analysis. For the final 20 min of the rest period, the cells were treated with the indicated concentration of MBCD at 37°C in loading buffer. The baseline level of Fluo-3 (FL-1) and Fura Red (FL-3) fluorescence was monitored using a FACScan I (BD Biosciences) and the CellQuest software package (BD Biosciences). The cells were then stimulated either with Ag (i.e., 10 nM PC-BSA) or 1 μg/ml of A23187 ionophore (Molecular Probes; catalog no. A-1493), and the level of fluorescence was monitored for an additional 2.5 min. The relative level of intracellular Ca^{2+} was determined by ratiometric analysis (i.e., FL-1/FL3) of the data using the FloJo software package (Treestar, San Carlos, CA).

Immunofluorescence microscopy

A20μWT B cells pulsed with ligand (i.e., CTB-FITC, PC-KLH-DIG, $F(ab')_2$ of rabbit anti-human IgM (Jackson ImmunoResearch Laboratories, West Grove, PA; catalog no. 309-006-043) or biotinylated transferrin (Tf-btn (Sigma-Aldrich; catalog no. T3915)) as indicated were attached to coverslips, fixed, and permeabilized as previously reported (27). The cells were then stained with one or more of the following reagents as appropriate; sheep anti-DIG (Roche; catalog no. 1333089), followed by donkey anti-sheep IgG-Texas Red (Jackson ImmunoResearch Laboratories; catalog no. 713-076-147), donkey anti-rabbit IgG-Texas Red (Jackson ImmunoResearch Laboratories; catalog no. 711-076-152), SA-Texas Red (Jackson ImmunoResearch Laboratories; catalog no. 016-070-084), or rat anti-lysosome-associated membrane protein (anti-LAMP-2; GL2A7) (29) followed by donkey anti-rat IgG-Texas Red (Jackson ImmunoResearch Laboratories; catalog no. 712-076-153). Finally, all cells were stained with 1 μg/ml of 4′,6-diamidino-2-phenylindole (DAPI; Molecular Probes; catalog no. D-1306) before final washing and mounting with ProLong Antifade mounting medium (Molecular Probes; catalog no. P-7481).

Results

BCR-mediated Ag internalization occurs independently of plasma membrane lipid rafts

The kinetics of BCR-mediated Ag internalization have been extensively documented by multiple laboratories (26, 28–32). From this collection of studies it is known that BCR-mediated Ag internalization occurs with relatively rapid kinetics, such that a plateau of internalization is attained in as little as 15 min, at which point 50% or more of the total cell surface Ag-BCR complexes have been internalized. If plasma membrane lipid rafts represent the major pathway by which Ag-BCR complexes are internalized, then internalization of plasma membrane lipid rafts would be expected to occur with similar kinetics. Accordingly, we directly determined the kinetics of internalization of plasma membrane lipid rafts by A20μWT murine B lymphocytes.

CTB is a protein that specifically binds the head group of the GM_1 glycosphingolipid, which is known to be restricted to plasma membrane lipid raft (1). Therefore, by monitoring the internalization of CTB-HRP bound to the GM_1 component of cell surface lipid rafts, we should be able to determine the kinetics of internalization of these cell surface structures. To confirm that externally applied CTB specifically labels the plasma membrane lipid rafts of B lymphocytes, we directly followed the lipid raft partitioning of CTB-HRP bound to A20μWT B cells. Accordingly, CTB-HRP was bound to A20μWT B cells on ice, and unbound ligand was removed by washing. After a brief 5-min incubation at 37°C, the labeled cells were returned to ice and solubilized in ice-cold TNE buffer containing either 0.1 or 1% TX-100. Lipid rafts were then separated from the remainder of the detergent lysate by flotation on discontinuous sucrose density gradients, and the distribution of CTB-HRP within the gradient was determined. As shown in Fig. 1, CTB-HRP was most highly enriched within the lipid raft-containing region of the gradient, demonstrating that CTB-HRP selectively binds to GM_1-positive plasma membrane lipid rafts of A20μWT cells and, therefore, specifically labels these structures with HRP. Moreover, these results also demonstrate that in this system lipid raft integrity is best maintained using

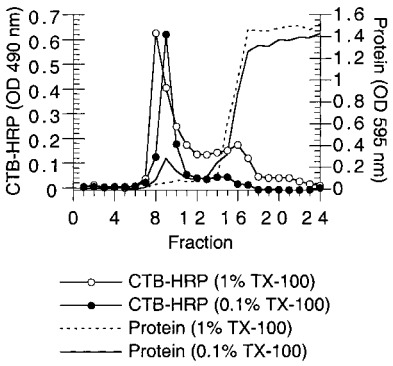

FIGURE 1. Lipid raft partitioning of CTB-HRP bound to A20μWT B cells. A20μWT B cells were labeled with CTB-HRP on ice and then warmed to 37°C for 5 min. The cells were chilled on ice and solubilized in ice-cold TNE containing either 1 or 0.1% TX-100. Lipid rafts were isolated by discontinuous sucrose density gradient centrifugation, and the distribution of CTB-HRP was determined via a colorometric assay for HRP activity. For cells lysed in TNE containing 0.1% TX-100, 95–100% of the total CTB-HRP was found in the lipid raft-containing region of the gradient (i.e., gradient fractions 8–10, which contain the 5/35% sucrose interface). For cells lysed in TNE containing 1% TX-100, between 65 and 90% of the CTB-HRP was found in the lipid raft-containing region of the gradient. Moreover, only in gradients of cell lysed in 0.1% TX-100 was a high level of cellular protein reproducibly detected in the lipid raft region of the gradient. Shown are the results from one representative experiment of three.

a low concentration of detergent (i.e., 0.1% TX-100) during cell lysis.

Using these same conditions of CTB-HRP binding followed by a colorometric assay to track the internalization of HRP-labeled ligands (28), we determined the kinetics of lipid raft-mediated CTB-HRP internalization. As shown in Fig. 2, lipid raft-associated CTB-HRP was internalized with kinetics markedly different from those of BCR-mediated Ag internalization, which have been previously reported (26–28, 31, 32) and are presented again in Fig. 5*A*. Specifically, a plateau of lipid raft-mediated CTB internalization was attained only after 30 min of incubation at 37°C, whereas BCR-mediated Ag internalization plateaued in as little as 15 min. Moreover, the plateau level of lipid raft-mediated endocytosis occurred at a point when only 20% of the total lipid raft-associated CTB-HRP was internalized, whereas Ag endocytosis plateaued at a level of 50% internalization or more. Furthermore, the kinetics of lipid raft-mediated CTB-HRP internalization were essentially identical with the published internalization kinetics for ligands bound to either of two lipid raft resident GPI-linked proteins (i.e., CD59 (9) and a mutant GPI-linked BCR (Ref. 25 and our unpublished observations)) in T cells and B cells, respectively. Finally, the differences in the kinetics of BCR-mediated Ag internalization vs lipid raft-mediated CTB-HRP internalization exactly mirror the published differences between the kinetics of clathrin-coated pit-mediated internalization of the TCR vs lipid raft-mediated internalization of CD59 in T lymphocytes (9), strongly suggesting that each of these phenomena occurs via a distinct mechanism.

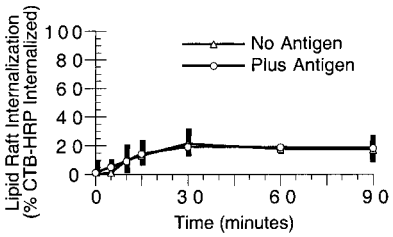

FIGURE 2. Kinetics of endocytosis of CTB-HRP. CTB-HRP was bound to cell surface plasma membrane lipid rafts of A20μWT cells on ice in the presence or the absence of unlabeled Ag (i.e., 1 μM PC-BSA). The cells were subsequently washed and warmed to 37°C for the indicated times, and the distribution of cell-associated CTB-HRP was determined using a colorometric assay for HRP activity as previously reported (28). Shown is the fraction of total cell-associated CTB-HRP detected within intracellular compartments at each time point. In the absence of BCR-bound Ag, lipid raft-bound CTB-HRP was internalized with relatively slow kinetics such that ~20% of the total raft-associated CTB was internalized after 30 min of incubation. Addition of unlabeled Ag (i.e., PC-BSA), which induced internalization of 60–80% of cell surface BCR molecules by 15 min of incubation (Fig. 4 as well as data not shown), did not detectably alter the kinetics of CTB-HRP internalization. Shown is the average level of CTB-HRP internalization from three independent experiments. The bars indicate the range of experimental values obtained for all samples throughout all of the experiments. The bar for the 60 min time point is smaller than the icon.

While the results presented above demonstrate that the kinetics of BCR-mediated Ag internalization and lipid raft-mediated CTB-HRP internalization are distinct, they do not address the possibility that Ag-BCR complexes, once formed, may translocate into plasma membrane lipid rafts and induce more rapid and/or extensive lipid raft internalization. To address this possibility, the effect of Ag-induced stimulation of BCR internalization on the kinetics of lipid raft internalization was analyzed. To accomplish this, we took advantage of the published observation that cross-linking of the PC-specific BCR of A20μWT B cells by polyvalent Ag (i.e., PC-BSA) induces rapid and extensive BCR internalization (27). Accordingly, the kinetics of lipid raft-mediated CTB-HRP internalization by A20μWT cells exposed to PC-BSA were determined. As shown in Fig. 2, induction of BCR internalization by the binding of PC-BSA fails to detectably affect the kinetics of lipid raft-mediated CTB-HRP internalization. These results demonstrate that upon formation, cell surface Ag-BCR complexes fail to enter a large fraction of plasma membrane lipid rafts and alter their kinetics of internalization. However, these results do not rule out the possibility that Ag-BCR internalization may be mediated by only a small fraction of cell surface lipid rafts. If this is the case, even extensive Ag-BCR partitioning into rafts and subsequent internalization may not detectably alter the kinetics of internalization of the entire population of cell surface lipid rafts. Therefore, to address this possibility we determined the level of Ag-BCR partitioning into plasma membrane lipid rafts during the period of rapid Ag-BCR internalization. Even if Ag-BCR complex internalization is mediated only by a small fraction of plasma membrane lipid rafts, a high level of Ag-BCR partitioning into lipid rafts would be expected during periods of rapid and extensive Ag-BCR internalization. Accordingly, we used labeled Ag (i.e., PC-BSA-HRP) to ascertain the extent of lipid raft partitioning of Ag-BCR complexes during the period of rapid Ag-BCR complex internalization. As shown in *A* and *B* of Fig. 3, after either 5 or 15 min of incubation at 37°C (times at which rapid and extensive BCR-mediated PC-BSA-HRP internalization is occurring (27)) only a small fraction (i.e., 5%) of the total cell-associated Ag-BCR complexes was present within isolatable lipid rafts. Moreover, this level of Ag-BCR partitioning into plasma membrane lipid rafts was observed even in cells maintained on ice, suggesting that either translocation of Ag-BCR complexes into rafts can occur at low temperature or that Ag may directly bind to BCR molecules preexisting within lipid rafts. Finally, even when we used anti-BCR Abs to induce conditions of additional Ag-BCR complex cross-linking (conditions that have been reported to result in more extensive BCR partitioning into lipid rafts in these cells (22)), we

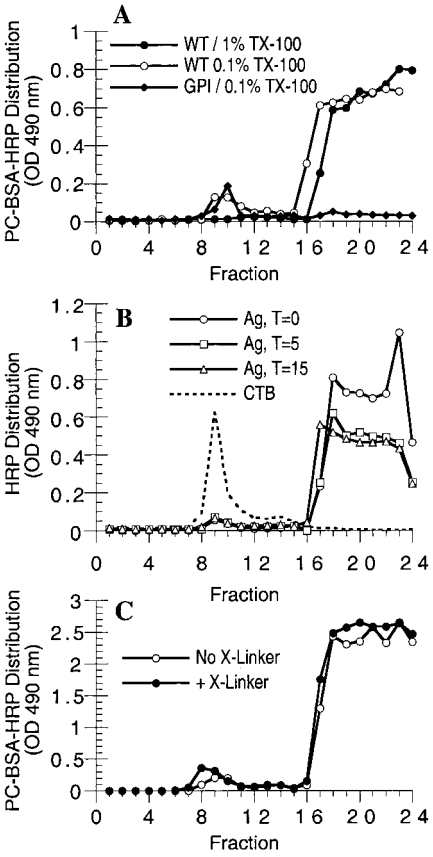

FIGURE 3. Lipid raft partitioning of PC-BSA-HRP bound to the human IgM BCR of A20μWT. *A*, Labeled Ag (i.e., PC-BSA-HRP) was bound to the cell surface PC-specific human IgM BCRs of A20μWT or A20μPI cells on ice. The cells were then washed and warmed to 37°C for 5 min to allow high levels of BCR-mediated PC-BSA-HRP internalization to occur. The cells were chilled on ice and lysed in TNE containing the indicated amount of TX-100, and lipid rafts were isolated by sucrose density gradient centrifugation. When A20μWT cells were lysed in 1% TX-100, the lipid raft region of the gradient contained an average of 0.8% of the total cell-associated Ag (the values for the individual experiments were 1, 0.4, and 1%). However, when A20μWT cells were lysed in 0.1% TX-100, the lipid raft region of the gradient contained an average of 5% of the total cell-associated Ag (the values for the individual experiments were 7, 5, and 3%). When the gradients from A20μPI cells were analyzed, the bulk of the PC-BSA-HRP was found in the lipid raft-containing region of the gradient. In all experiments the control gradient of cells pulsed with CTB-HRP gave results similar to those illustrated in Fig. 1, assuring that the lipid raft isolation protocol was working properly (results not shown). Shown are representative results from one of three (A20μWT) or four (A20μPI) independent experiments. *B*, PC-BSA-HRP was bound to A20μWT cells as in *A*. The cells were then incubated for 0, 5, or 15 min at 37°C before detergent lysis and analysis of the lipid raft partitioning of BCR-associated Ag by sucrose density gradient centrifugation. To confirm the expected migration of plasma membrane lipid rafts in this experiment, CTB-HRP was used in place of Ag in a parallel sample. In all the experiments performed, no differences were observed in the level of PC-BSA-HRP within the lipid raft-containing region of the gradient from samples incubated for different periods of time at 37°C. The decreased amount of Ag detected in the non-raft-containing region of the gradient for the 5 and 15 min samples is consistent with the low level of Ag "shedding" observed upon incubation of the cells at 37°C (27) Shown are representative results for one of three independent experiments. *C*, PC-BSA-HRP was bound to A20μWT cells as in *A*. However, in the experimental sample the resulting Ag-BCR complexes were more extensively cross-linked by the addition of 0.1 μM F(ab′)$_2$ of rabbit anti-human IgM. After subsequent incubation for 5 min at 37°C, the cells were lysed in TNE/0.1% TX-100, lipid rafts were isolated, and the distribution of PC-BSA-HRP was determined as in *A*. Shown are the results from one of two independent experiments performed completely independent of the experiments used to generate the plot shown in *A*. In both experiments additional Ag-BCR cross-linking resulted in an approximate doubling of the fraction of Ag-BCR complexes found in the lipid raft-containing region of the gradient.

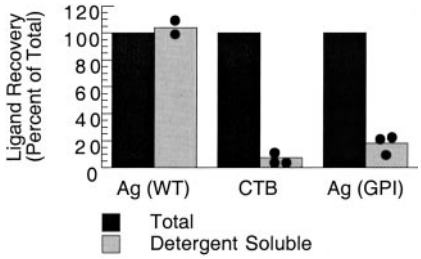

FIGURE 4. Differential recovery of CTB-HRP and PC-BSA-HRP in detergent lysates of A20μWT and A20μPI B cells. PC-BSA-HRP or CTB-HRP was bound to A20μWT or A20μPI B cells as described in Figs. 1 and 3. The cells were then washed to remove unbound ligand and resuspended in ice-cold 0.1% TX-100. Fifty microliters of the sample was removed immediately and used to measure total cell-associated ligand. After incubation for 30 min on ice to allow solubilization of the cells and release of lipid rafts, the sample was centrifuged to pellet the detergent-insoluble material (as was performed for normal preparation of the samples for sucrose density gradient centrifugation). After centrifugation, 50 μl of the supernatant was removed to determine the level of detergent-soluble ligand. Interestingly, while all the cell-associated PC-BSA-HRP bound to the WT BCR (Ag (WT)) was recovered in the detergent-soluble supernatant, only 7% of the CTB-HRP bound to plasma membrane lipid rafts and 18% of the PC-BSA-HRP bound to the lipid raft-resident GPI-linked BCR (Ag (GPI)) were found to be detergent soluble. The bars represent the average percent recovery of Ag or CTB for all experiments. The data points represent the values obtained from each independent experiment.

observed only a slight increase in the fraction of cell surface Ag-BCR complexes present within isolatable lipid rafts (Fig. 3*C*).

Another possible explanation for the observed low level of Ag-BCR partitioning into lipid rafts could be the loss of Ag-BCR-containing lipid rafts during preparation of the experimental sample. To determine whether this was the case, we analyzed the level of recovery of BCR-associated PC-BSA-HRP in the detergent cell lysates used to generate the gradient profiles presented in Fig. 3. As illustrated in Fig. 4, all the cell-associated Ag-BCR complexes were recovered in the detergent lysate that was used to analyze the lipid raft partitioning of these complexes, demonstrating that the observed low level of raft partitioning of the Ag-BCR complexes is not due to the loss of lipid raft-associated Ag-BCR complexes during sample preparation. Interestingly, when we analyzed the recovery of lipid raft-associated CTB-HRP under the same experimental conditions, we observed a profound (i.e., >90%) loss of cell-associated CTB-HRP from the cleared detergent lysates. Importantly, while this experimental finding is consistent with the documented association between plasma membrane lipid rafts and detergent-insoluble aspects of the cytoskeleton (5), it is inconsistent with the extensive partitioning of Ag-BCR complexes into GM_1-positive lipid rafts for subsequent internalization, since this scenario would be expected to result in a significant level of loss of PC-BSA-HRP from cleared detergent lysates (analogous to that observed for the lipid raft-bound CTB-HRP). Moreover, these results raise the possibility that the Ag-BCR complexes found in the lipid raft-containing region of the sucrose gradients (Fig. 3) may be present in GM_1-negative lipid rafts. Thus, while the observed level of lipid raft partitioning of cell surface Ag-BCR complexes would

be sufficient to mediate lipid raft-based generation of intracellular second messenger molecules, it is unlikely to be sufficient to mediate the extensive level of Ag-BCR internalization that is known to occur during the first 15–30 min of incubation at 37°C.

Another possible explanation for the observed low level of lipid raft partitioning of Ag-BCR complexes could be dissociation of labeled Ag from lipid raft-resident BCR molecules. To determine whether this was the case, we examined the lipid raft partitioning of PC-BSA-HRP bound to the GPI-linked PC-specific BCR of A20μPI B cells, since the GPI-linked BCR expressed by these cells has been demonstrated to constitutively partition into plasma membrane lipid rafts (25). As illustrated in Fig. 4, upon detergent solubilization of the A20μPI cells, 82 ± 8.2% of the total PC-BSA-HRP bound to the GPI-linked BCR was lost to the detergent-insoluble pellet. This result is analogous to the profound loss of lipid raft-associated CTB-HRP observed at this step in the protocol and is in direct contrast to the complete recovery of PC-BSA-HRP bound to the normal BCRs of A20μWT B cells. Moreover, when the detergent-soluble material from A20μPI cells was run on a sucrose gradient to separate raft from non-raft material, the majority of the labeled Ag applied to the gradient was found in the region of the gradient containing lipid rafts (Fig. 3*A*). Taken together, these results demonstrate that the vast majority of the PC-BSA-HRP bound to the GPI-linked BCR of A20μPI cells partitioned into plasma membrane lipid rafts (i.e., it was either lost in the detergent-insoluble material or banded at the 5/30% sucrose interface), Since the Ag binding site of the PC-specific BCRs expressed by A20μWT and A20μPI B cell lines is identical, these results demonstrate that the low level of lipid raft partitioning of Ag-BCR complexes in A20μWT cells is not due to dissociation of the Ag from the WT BCR during the course of the experiment.

Consequently, the only remaining scenario by which plasma membrane lipid rafts may be involved in the rapid and extensive internalization of a large portion of Ag-BCR complexes is if internalization of Ag-BCR complexes occurs very rapidly after entry of the complexes into lipid rafts, followed by rapid and efficient removal of Ag-BCR complexes from lipid rafts soon after delivery to early endocytic compartments. However, if this is the case, it would be expected that disruption of plasma membrane lipid rafts by extraction of cellular cholesterol (1) would dramatically alter the kinetics of Ag-BCR internalization. Accordingly, we determined the effect of lipid raft disruption on the rate and extent of Ag-BCR internalization. To disrupt the plasma membrane lipid rafts of A20μWT B cells, cells were treated with MBCD to extract cellular cholesterol (22, 33). As illustrated in Fig. 5*A*, the rate and extent of Ag-BCR complex internalization were unaffected by MBCD treatment of A20μWT cells. To demonstrate that MBCD treatment of A20μWT cells resulted in disruption of plasma membrane lipid rafts, we analyzed the effect of MBCD treatment on the kinetics of lipid raft-mediated CTB internalization. However, we discovered that MBCD treatment of A20μWT cells resulted in a dose-dependent and selective inhibition of CTB binding. Specifically, while treatment of A20μWT cells with any concentration of MBCD up to and including 5 mM failed to detectably alter the level of Ag binding (i.e., the level of Ag binding to drug-treated cells was always between 90 and 100% of that observed to non-MBCD-treated cells), treatment of cells with MBCD resulted in a dose-dependent decrease in CTB binding such that at 5 mM MBCD, CTB binding was decreased by half (i.e., the level of CTB binding to 5 mM MBCD-treated cells was decreased by 45, 44, and 54% in three independent experiments). Because the decreased binding of CTB to MBCD-treated cells made analysis of CTB internalization in these cells technically difficult, we directly analyzed the effect of MBCD treatment on the partitioning of Ag-BCR

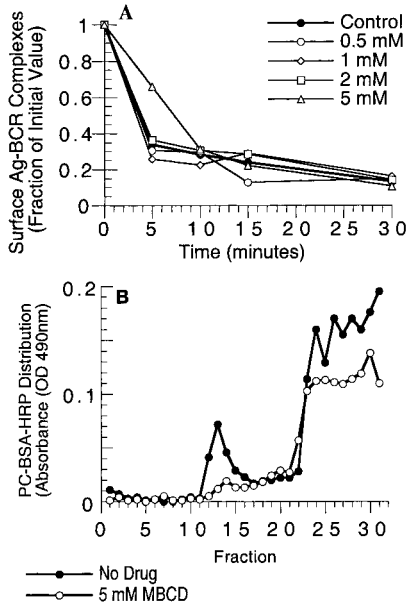

FIGURE 5. Effect of lipid raft disruption on the kinetics of BCR-mediated Ag internalization. *A*, The lipid rafts of A20μWT cells were disrupted by depletion of cellular cholesterol with the indicated concentration of MBCD. Ag (i.e., PC-KLH-btn) was then bound to the PC-specific IgM BCR of the treated cells on ice. After washing, the cells were warmed to 37°C for the indicated times, and the level of remaining cell surface Ag was determined by staining with SA-FITC and analysis by flow cytometry. Shown is the fraction of initially bound Ag remaining at the surface of viable (i.e., propidium iodide-negative) cells. Under these conditions we have determined that <10% of the bound Ag is released from the cells upon incubation at 37°C. Importantly, MBCD treatment has no significant effect on the initial level of Ag binding. The only data point that exhibited any notable difference in this experiment was the extent of Ag-BCR internalization in 5 mM MBCD-treated cells after 5 min of incubation at 37°C. However, this was not a reproducible experimental finding and (due to the modest level of cell death observed with this level of MBCD treatment) is likely to represent an experimental artifact. Shown are representative results from one of seven independent experiments. *B*, PC-BSA-HRP was bound to A20μWT cells as described in Fig. 3. The cells were then divided into two equal samples and incubated for 30 min at 37°C in either buffer or buffer containing 5 mM MBCD. (The cells were MBCD treated after Ag binding because we determined that pretreatment with MBCD made the cells so sensitive to centrifugation that the multiple washes necessary to remove unbound ligand killed >50% of the cells.). The samples were then lysed in ice-cold 0.1% TX-100, and the partition of BCR-associated PC-BSA-HRP into lipid rafts was determined as in Fig. 3. Illustrated are representative results from one of three independent experiments demonstrating that MBCD treatment profoundly decreases the level of Ag-BCR complexes present within biochemically isolatable lipid rafts.

complexes into plasma membrane lipid rafts. As illustrated in Fig. 5*B*, treatment of A20μWT cells with 5 mM MBCD profoundly decreased the level of BCR-associated Ag detected within the lipid raft-containing region of the sucrose density gradient, directly demonstrating that MBCD treatment decreases the detergent stability of the cell surface lipid rafts into which the Ag-BCR complexes partition. To further extend these results and demonstrate that MBCD treatment inhibits lipid raft function in intact cells, we analyzed the effect of MBCD treatment on the ability of PC-BSA binding to the PC-specific BCR of A20μWT cells to elicit an intracellular Ca^{2+} response (34). While the precise mechanism by which lipid raft disruption alters the BCR-induced intracellular Ca^{2+} response in A20 cells is a matter of debate (35), the results presented in Fig. 6 demonstrate an MBCD dose-dependent alteration in the characteristics of the BCR-induced intracellular Ca^{2+}

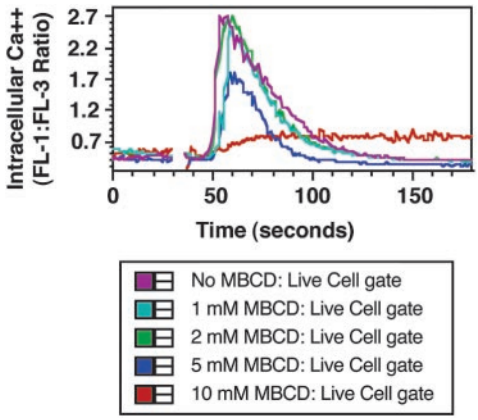

FIGURE 6. MBCD treatment disrupts lipid rafts and alters the intracellular Ca^{2+} response to Ag-induced BCR signaling. A20μWT cells were loaded with the Ca^{2+}-sensitive dyes Fluo-3 and Fura Red and then treated with the indicated amounts of MBCD for 30 min at 37°C. The baseline level of intracellular free calcium (which is reflected in the ratio of Fluo-3 (FL-1) to Fura Red (FL-3) fluorescence) was established for each sample before stimulation with PC-BSA (in the continued presence of MBCD) and continued monitoring of cellular fluorescence. The results demonstrate that treatment with 5 mM MBCD (a concentration of drug that did not alter BCR-mediated Ag internalization (Fig. 5*A*) blunted the Ag-induced BCR-mediated intracellular calcium response. The intracellular Ca^{2+} response of A20μWT cells stimulated with the Ca^{2+} ionophore A23187 was not altered by treatment with MBCD. Shown are representative results from one of four independent experiments.

response of MBCD-treated A20μWT cells. Together, these results demonstrate that the rate and extent of rapid Ag-BCR complex internalization are unaffected by extensive disruption of plasma membrane lipid rafts. This result as well as those presented in Figs. 1–4 are consistent with the idea that plasma membrane lipid rafts are not an obligatory structure for the rapid and extensive internalization of the bulk of cell surface Ag-BCR complexes.

Differential intracellular trafficking of internalized Ag-BCR complexes and internalized plasma membrane lipid rafts

While the results presented above demonstrate that residence within plasma membrane lipid rafts is not an obligatory step on the pathway of internalization of the bulk of cell surface Ag-BCR complexes, they do not rule out the possibility that a small portion (e.g., 5–10%) of Ag-BCR complexes may be internalized while resident within lipid rafts. Moreover, if these rafts and their resident Ag-BCR complexes traffick as a unit, they might be expected to be restricted to the early aspects of the endocytic pathway, as observed for internalized lipid rafts in other cells (6, 7). This would be in stark contrast to the bulk of the internalized Ag-BCR complexes, which are known to be delivered to late endocytic compartments for processing and degradation (27). We therefore compared the intracellular trafficking of the bulk of the internalized Ag-BCR complexes to that of internalized plasma membrane lipid rafts.

Since it is presently not possible to selectively label only those BCR molecules within lipid rafts, we were forced to compare the intracellular distribution of internalized Ag-BCR complexes (the majority of which are internalized via a non-lipid raft-dependent pathway) to the intracellular distribution of internalized CTB that is brought into the cell via lipid raft-mediated internalization. As shown in Fig. 7 (*A* and *B*), the intracellular distribution of BCR-internalized Ag and anti-BCR Abs is notably different from the intracellular distribution of lipid raft-internalized CTB. While some endocytic vesicles (most likely early endosomes) contain

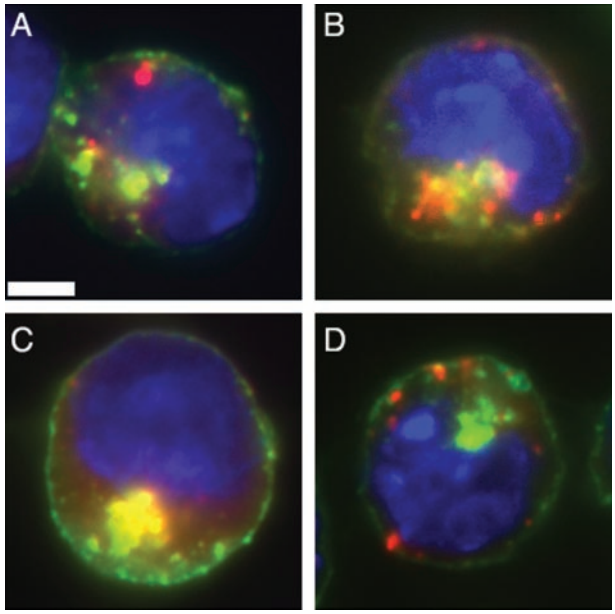

FIGURE 7. IFM localization of lipid raft-internalized CTB vs BCR-internalized Ag. *A*, Both CTB-FITC and Ag (PC-BSA-DIG) were bound to the surface of A20μWT B cells on ice, and unbound ligand was washed away. The labeled cells were warmed to 37°C for 30 min to allow internalization to occur. The cells were then fixed, permeabilized, and stained with sheep anti-DIG Ab, followed by donkey anti-sheep IgG-Texas Red. The cells were also stained with DAPI. CTB-FITC was present both at the cell surface as well as within a juxtanuclear cluster of intracellular vesicles. BCR-internalized Ag was found predominantly within intracellular vesicles not containing detectable levels of CTB-FITC. *B*, Both CTB-FITC as well as $F(ab')_2$ of rabbit anti-human IgM were bound and internalized as in *A*. The cells were then fixed, permeabilized, and stained with donkey anti-rabbit IgG-Texas Red as well as DAPI. As in *A*, CTB-FITC was found within a juxtanuclear aggregate of vesicles. Similar to BCR-internalized Ag, some of the BCR-internalized anti-BCR Ab was found within endocytic vesicles lacking detectable amounts of internalized CTB-FITC (red staining). However, some of the internalized anti-BCR Ab was found within CTB-FITC-containing endocytic compartments (yellow staining). However, in neither case did BCR-internalized Ag or anti-BCR Abs exhibit 100% colocalization with lipid raft-internalized CTB-FITC. *C*, A20μWT cells that had bound and internalized CTB-FITC as well as Tf-btn were fixed, permeabilized, and stained with SA-Texas Red (to localize Tf-btn) as well as DAPI. Analysis of the cells revealed a considerable level of colocalization of internalized CTB and Tf (yellow staining) within early and recycling endosomes. *D*, A20μWT B cells that were allowed to bind and internalize CTB-FITC were fixed, permeabilized, and stained for the late endosome/lysosome marker LAMP-2 (using the rat mAb GL2A7, followed by anti-rat IgG-Texas Red) as well as with DAPI. The staining revealed that lipid raft-internalized CTB was not delivered to LAMP-2-positive late endocytic compartments. Shown are representative results from one of three independent experiments in which the vast majority of the cells exhibited a staining pattern similar to that presented in this figure. The bar in *A* equals 5 μm. All images were taken at the same magnification.

ligands internalized via both pathways (these vesicles are especially apparent in Fig. 7*B*), a large portion of BCR-internalized ligands are present within intracellular compartments that do not contain detectable levels of lipid raft-internalized CTB. Moreover, internalized lipid rafts, unlike internalized Ag-BCR complexes, were repeatedly observed to be localized to a juxtanuclear aggregate of intracellular vesicles reminiscent of Golgi complex-associated recycling endosomes (36). To determine whether lipid raft-internalized CTB is actually restricted to early and recycling endocytic compartments, we compared the intracellular distribution of internalized CTB to the distribution of internalized Tf as

well as the late endosome and lysosome marker LAMP-2 (27). As shown in Fig. 7, lipid raft-internalized CTB exhibits a high degree of colocalization with internalized Tf within early and recycling endosomes (Fig. 7*C*), but little if any colocalization with LAMP, which marks the latter aspects of the endocytic pathway (Fig. 7*D*). Importantly, while these results do not prove that Ag-BCR complexes and lipid raft-associated CTB are internalized by distinct endocytic pathways (e.g., clathrin-coated pits vs caveolae-like structures), since the same relative intracellular distribution could be attained by either cointernalization and subsequent sorting within endocytic compartments or rapid degradation of CTB-FITC upon delivery to late endocytic compartments, they are consistent with the localization of internalized lipid rafts to early and recycling endocytic compartments in B lymphocytes, mirroring the trafficking pathway of internalized lipid rafts in other cell types (6, 7) and are in contrast to the delivery of internalized Ag-BCR complexes to late endocytic compartments (27).

In total, the results presented in this report are consistent with the hypothesis that the bulk of Ag-BCR complex internalization occurs via a pathway independent of plasma membrane lipid rafts. Moreover, the results are consistent with the possibility that Ag-BCR complexes that are internalized while resident within plasma membrane lipid rafts may have a different intracellular itinerary than the bulk of the Ag-BCR complexes internalized via plasma membrane clathrin-coated pits.

Discussion

The BCR has two functions upon binding of cognate Ag. One is signal transduction and generation of intracellular second messenger molecules. The second is to mediate Ag internalization and delivery to intracellular compartments for processing and subsequent presentation on MHC class II molecules. While plasma membrane lipid rafts are critically involved in BCR-mediated signal transduction (2–4), the role of lipid rafts in endocytosis, processing, and presentation of cognate Ag is less clear.

In this report we directly demonstrated that CTB-HRP-labeled lipid rafts on the surface of A20 B cells are internalized with kinetics distinct from those of the bulk of the Ag-BCR complexes. Moreover, we demonstrate that induction of rapid and extensive BCR internalization fails to alter the kinetics of lipid raft-mediated CTB-HRP internalization. This result is in apparent contrast to the results of Cheng and colleagues (22), who demonstrate that in the CH27 B cell line, anti-BCR-induced internalization of cell surface BCR molecules results in an increase in the CTB-HRP-catalyzed diaminobenzidene (DAB)-mediated cross-linking of Tf receptor (TfR) and newly synthesized MHC class II molecules, a result that the authors interpreted as suggesting that induction of BCR internalization by the binding of polyvalent ligand alters the internalization of GM_1-containing lipid rafts. However, the DAB-mediated cross-linking protocol used in these experiments is relatively complex in design, making it difficult to determine whether the observed cross-linking is occurring within intracellular endocytic compartments or at the cell surface. This potential problem is especially acute in the case of the TfR-based experiments where the cohort of TfR molecules being followed was initially present only at the surface of the cell (where they were labeled with amino-reactive biotin), but which may have redistributed to intracellular compartments upon warming of the cells to 37°C to allow for BCR and lipid raft internalization. In fact, in these experiments the reported decrease in DAB-mediated TfR-btn cross-linking in cells incubated at 37°C may be the result of the rapid internalization of TfR-btn from the cell surface, removing it from the domain of cell surface CTB-HRP-catalyzed DAB-mediated cross-linking. In the case of our direct assessment of lipid raft-mediated CTB-HRP internalization, these types of confounding issues are not applicable, making interpretation of the experimental results simpler and more direct. Moreover, our direct measurements of the kinetics of CTB-HRP-labeled lipid raft internalization are consistent with published results on the kinetics of internalization of lipid raft-resident GPI-linked proteins in both the murine A20 B cell line (26) and other lymphocytes (9, 24).

The second finding in our report that appears at odds with the published literature is our finding that upon binding of Ag, only a small fraction (i.e., 5%) of cell surface Ag-BCR complexes are found within lipid rafts (Fig. 3). Moreover, our kinetic analysis suggests that either this minor fraction of Ag-BCR complexes translocates into lipid rafts at reduced temperature or that some cell surface BCR molecules are constitutively associated with lipid rafts. This is in apparent contrast to the results presented in Fig. 1 of the report by Cheng and colleagues (22) that demonstrates an apparent translocation of cell surface BCR molecules into lipid rafts upon binding of anti-BCR Abs. However, the results presented in Fig. 4*A* of the same report demonstrate the partitioning of Ag-BCR complexes into lipid rafts at reduced temperature and, furthermore, show that the level of raft partition of Ag-BCR complexes does not change with incubation at 37°C. Moreover, while the results presented in Fig. 4*A* (22) suggest a relatively high level of Ag-BCR partitioning into lipid rafts, the results presented in Fig. 4*B* of the same figure suggest a level of lipid raft partitioning closely approximating that which we have observed in our experimental system (i.e., 15–30%). Thus, while the precise level of Ag-BCR complexes partitioning into plasma membrane lipid rafts may be highly dependent upon the specific conditions of Ag binding, the results presented in this report extend the findings of Cheng et al. (22) by demonstrating that while internalization of lipid raft-resident Ag-BCR complexes is likely to occur, lipid raft-mediated internalization is not the major pathway by which the bulk of Ag-BCR complexes gain access to the endocytic pathway of the cell nor is partitioning into lipid rafts an obligatory step on the pathway of internalization of the bulk of cell surface Ag-BCR complexes. Importantly, this result is consistent with the observation that mutant GPI-linked BCR molecules that are highly restricted to plasma membrane lipid rafts mediate significantly less efficient Ag processing and presentation than the wild-type transmembrane BCR, which is known to efficiently access late endocytic compartments (25). The decrease in the efficiency of Ag processing via the GPI-linked BCR (which fails to associated with the CD79 α/β dimmer) could be due to either changes in intracellular signaling due to the absence of the immunoreceptor tyrosine-based activation motifs within the cytoplasmic tails of the CD79 subunits or altered endocytosis and intracellular trafficking due to the absence of potential tyrosine-based endocytosis motifs within the cytoplasmic tails of the CD79 subunits of the BCR. This proposed scenario raises the question of the possible function of lipid raft-mediated internalization of Ag-BCR complexes. Presently, we feel that the most likely function of the internalization of lipid raft-associated Ag-BCR complexes could be to alter BCR signaling occurring from within these structures. Presently, our laboratory is pursuing experiments to test this hypothesis.

References

1. Brown, D. A., and E. London. 2000. Structure and function of sphingolipid- and cholesterol-rich membrane rafts. *J. Biol. Chem. 275:17221.*
2. Langlet, C., A. M. Bernard, P. Drevot, and H. T. He. 2000. Membrane rafts and signaling by the multichain immune recognition receptors. *Curr. Opin. Immunol. 12:250.*
3. Aman, M. J., and K. S. Ravichandran. 2000. A requirement for lipid rafts in B cell receptor induced Ca^{2+} flux. *Curr. Biol. 10:393.*

4. Petrie, R. J., P. P. Schnetkamp, K. D. Patel, M. Awasthi-Kalia, and J. P. Deans. 2000. Transient translocation of the B cell receptor and Src homology 2 domain-containing inositol phosphatase to lipid rafts: evidence toward a role in calcium regulation. *J. Immunol. 165:1220.*
5. Ikonen, E. 2001. Roles of lipid rafts in membrane transport. *Curr. Opin. Cell Biol. 13:470.*
6. Nichols, B. J., A. K. Kenworthy, R. S. Polishchuk, R. Lodge, T. H. Roberts, K. Hirschberg, R. D. Phair, and J. Lippincott-Schwartz. 2001. Rapid cycling of lipid raft markers between the cell surface and Golgi complex. *J. Cell Biol. 153:529.*
7. Chatterjee, S., E. R. Smith, K. Hanada, V. L. Stevens, and S. Mayor. 2001. GPI anchoring leads to sphingolipid-dependent retention of endocytosed proteins in the recycling endosomal compartment. *EMBO J. 20:1583.*
8. Fra, A. M., E. Williamson, K. Simons, and R. G. Parton. 1994. Detergent-insoluble glycolipid microdomains in lymphocytes in the absence of caveolae. *J. Biol. Chem. 269:30745.*
9. Deckert, M., M. Ticchioni, and A. Bernard. 1996. Endocytosis of GPI-anchored proteins in human lymphocytes: role of glycolipid-based domains, actin cytoskeleton, and protein kinases. *J. Cell Biol. 133:791.*
10. Salisbury, J. L., J. S. Condeelis, and P. Satir. 1980. Role of coated vesicles, microfilaments, and calmodulin in receptor-mediated endocytosis by cultured B lymphoblastoid cells. *J. Cell Biol. 87:132.*
11. Miettinen, H. M., J. K. Rose, and I. Mellman. 1989. Fc receptor isoforms exhibit distinct abilities for coated pit localization as a result of cytoplasmic domain heterogeneity. *Cell 58:317.*
12. Amigorena, S., C. Bonnerot, J. R. Drake, D. Choquet, W. Hunziker, J. G. Guillet, P. Webster, C. Sautes, I. Mellman, and W. H. Fridman. 1992. Cytoplasmic domain heterogeneity and functions of IgG Fc receptors in B lymphocytes. *Science 256:1808.*
13. Bourguignon, L. Y., K. Balazovich, S. J. Suchard, O. Hindsgaul, and M. Pierce. 1986. Endocytosis of mannose-6-phosphate binding sites by mouse T-lymphoma cells. *J. Cell. Physiol. 127:146.*
14. Reid, P. A., and C. Watts. 1992. Constitutive endocytosis and recycling of major histocompatibility complex class II glycoproteins in human B-lymphoblastoid cells. *Immunology 77:539.*
15. Pelchen-Matthews, A., R. P. da Silva, M. J. Bijlmakers, N. Signoret, S. Gordon, and M. Marsh. 1998. Lack of $p56^{lck}$ expression correlates with CD4 endocytosis in primary lymphoid and myeloid cells. *Eur. J. Immunol. 28:3639.*
16. Pitcher, C., S. Honing, A. Fingerhut, K. Bowers, and M. Marsh. 1999. Cluster of differentiation antigen 4 (CD4) endocytosis and adaptor complex binding require activation of the CD4 endocytosis signal by serine phosphorylation. *Mol. Biol. Cell 10:677.*
17. Chuang, E., M. L. Alegre, C. S. Duckett, P. J. Noel, M. G. Vander Heiden, and C. B. Thompson. 1997. Interaction of CTLA-4 with the clathrin-associated protein AP50 results in ligand-independent endocytosis that limits cell surface expression. *J. Immunol. 159:144.*
18. Schneider, H., M. Martin, F. A. Agarraberes, L. Yin, I. Rapoport, T. Kirchhausen, and C. E. Rudd. 1999. Cytolytic T lymphocyte-associated antigen-4 and the TCRζ/CD3 complex, but not CD28, interact with clathrin adaptor complexes AP-1 and AP-2. *J. Immunol. 163:1868.*
19. Schneider, H., and C. E. Rudd. 2000. Tyrosine phosphatase SHP-2 binding to CTLA-4: absence of direct YVKM/YFIP motif recognition. *Biochem. Biophys. Res. Commun. 269:279.*
20. Bradshaw, J. D., P. Lu, G. Leytze, J. Rodgers, G. L. Schieven, K. L. Bennett, P. S. Linsley, and S. E. Kurtz. 1997. Interaction of the cytoplasmic tail of CTLA-4 (CD152) with a clathrin-associated protein is negatively regulated by tyrosine phosphorylation. *Biochemistry 36:15975.*
21. Dietrich, J., X. Hou, A. M. Wegener, and C. Geisler. 1994. CD3 gamma contains a phosphoserine-dependent di-leucine motif involved in down-regulation of the T cell receptor. *EMBO J. 13:2156.*
22. Cheng, P. C., M. L. Dykstra, R. N. Mitchell, and S. K. Pierce. 1999. A role for lipid rafts in B cell antigen receptor signaling and antigen targeting. *J. Exp. Med. 190:1549.*
23. Brown, D., and G. L. Waneck. 1992. Glycosyl-phosphatidylinositol-anchored membrane proteins. *J. Am. Soc. Nephrol. 3:895.*
24. Keller, G. A., M. W. Siegel, and I. W. Caras. 1992. Endocytosis of glycophospholipid-anchored and transmembrane forms of CD4 by different endocytic pathways. *EMBO J. 11:863.*
25. Mitchell, R. N., A. C. Shaw, Y. K. Weaver, P. Leder, and A. K. Abbas. 1991. Cytoplasmic tail deletion converts membrane immunoglobulin to a phosphatidylinositol-linked form lacking signaling and efficient antigen internalization functions. *J. Biol. Chem. 266:8856.*
26. Mitchell, R. N., K. A. Barnes, S. A. Grupp, M. Sanchez, Z. Misulovin, M. C. Nussenzweig, and A. K. Abbas. 1995. Intracellular targeting of antigens internalized by membrane immunoglobulin in B lymphocytes. *J. Exp. Med. 181: 1705.*
27. Gondre-Lewis, T. A., A. E. Moquin, and J. R. Drake. 2001. Prolonged antigen persistence within nonterminal late endocytic compartments of antigen-specific B lymphocytes. *J. Immunol. 166:6657.*
28. Drake, J. R., E. A. Repasky, and R. B. Bankert. 1989. Endocytosis of antigen, anti-idiotype, and anti-immunoglobulin antibodies and receptor re-expression by murine B cells. *J. Immunol. 143:1768.*
29. Granger, B. L., S. A. Green, C. A. Gabel, C. L. Howe, I. Mellman, and A. Helenius. 1990. Characterization and cloning of lgp110, a lysosomal membrane glycoprotein from mouse and rat cells. *J. Biol. Chem. 265:12036.*
30. Lanzavecchia, A. 1985. Antigen-specific interaction between T and B cells. *Nature 314:537.*
31. Metezeau, P., I. Elguindi, and M. E. Goldberg. 1984. Endocytosis of the membrane immunoglobulins of mouse spleen B-cells: a quantitative study of its rate, amount and sensitivity to physiological, physical and cross-linking agents. *EMBO J. 3:2235.*
32. Watts, C., and H. W. Davidson. 1988. Endocytosis and recycling of specific antigen by human B cell lines. *EMBO J. 7:1937.*
33. Kilsdonk, E. P., P. G. Yancey, G. W. Stoudt, F. W. Bangerter, W. J. Johnson, M. C. Phillips, and G. H. Rothblat. 1995. Cellular cholesterol efflux mediated by cyclodextrins. *J. Biol. Chem. 270:17250.*
34. Shaw, A. C., R. N. Mitchell, Y. K. Weaver, J. Campos-Torres, A. K. Abbas, and P. Leder. 1990. Mutations of immunoglobulin transmembrane and cytoplasmic domains: effects on intracellular signaling and antigen presentation. *Cell 63:381.*
35. Awasthi-Kalia, M., P. P. Schnetkamp, and J. P. Deans. 2001. Differential effects of filipin and methyl-β-cyclodextrin on B cell receptor signaling. *Biochim. Biophys. Acta 287:77.*
36. Sheff, D. R., E. A. Daro, M. Hull, and I. Mellman. 1999. The receptor recycling pathway contains two distinct populations of early endosomes with different sorting functions. *J. Cell Biol. 145:123.*